The Kinetics of Association and Phosphorylation of IκB Isoforms by IκB Kinase 2 Correlate with Their Cellular Regulation in Human Endothelial Cells

Ralf Heilker, Felix Freuler, Miroslava Vanek, Ruth Pulfer, Tanja Kobel, Jürg Peter, Hans-Günter Zerwes, Hans Hofstetter, and Jörg Eder*

Novartis Pharma AG, CH-4002 Basel, Switzerland

Received January 29, 1999; Revised Manuscript Received March 16, 1999

ABSTRACT: Activation of the transcription factor NF-κB depends on the specific dual phosphorylation of its inhibitor protein IκB by the homologous cytokine-inducible IκB kinases 1 and 2 (IKK1/2). Various IκB isoforms exist: IκBα, IκBβ1/2 (two alternative splice variants), and IκBε. However, the individual relevance and the specific regulation of these isoforms is not well-understood. We have studied the direct interaction of recombinant IκBα, IκBβ1, IκBβ2, and IκBε with the recombinant homodimeric IKK2. Fluorescence-based active site titration revealed that each IKK2 dimer contains two binding sites for IκB. By using surface plasmon resonance analysis, we found that all IκB proteins interact with the IKK2 dimer following a noncooperative binding mechanism. Further, the four IκB proteins bind to the kinase with equilibrium dissociation constants (K_D) in the range of 50−300 nM; the association rate constants for all IκB isoforms with IKK2 were between 6.0×10^3 and 22.5×10^3 M^{-1} s^{-1}, and the dissociation rate constants were between 1.25×10^{-3} and 1.75×10^{-3} s^{-1}. This high-affinity binding suggests that the previously observed preassociation of all analyzed IκB proteins with the biochemically purified 700 kDa IκB kinase (IKK) complex is based on a direct enzyme−substrate association between the various IκB isoforms and the IKK proteins. The apparent catalytic efficiencies (k_{cat}/K_M) of IKK2 for IκBα, IκBβ1, IκBβ2, and IκBε were 22×10^3, 10×10^3, 5.4×10^3, and 8.5×10^3 s^{-1} M^{-1}, respectively, with K_M values ranging between 1.7×10^{-6} and 3.2×10^{-6} M and k_{cat} values ranging between 1.5×10^{-2} and 3.7×10^{-2} s^{-1}. The relative affinities and catalytic efficiencies of IKK2 for the IκB isoforms were also reflected by the kinetics observed for the TNF-induced, phosphorylation-dependent degradation of the α, β1, β2, and ε isoforms of IκB in human umbilical vein endothelial cells. Therefore, differential regulation of the IκB isoforms in some cell types is not a direct result of the IKK activity, but appears to be due to parallel events.

Tumor necrosis factor α (TNFα)[1] is a potent pro-inflammatory cytokine, which has been implicated in a number of pathological conditions. Many of its biological effects are mediated by the nuclear factor kappa B (NF-κB) (*1*, *2*). This transcription factor is composed of two subunits belonging to the Rel family of DNA-binding proteins (*3*). In nonstimulated cells, it is sequestered in the cytoplasm by a member of the inhibitor kappa B (IκB) family. After the cells are stimulated with TNFα, IκB is phosphorylated by a specific IκB kinase activity on two N-terminal serine residues which are arranged in an SxxxS motif for the α, β, and ε isoforms of IκB (*4*−*8*). Following this dual phosphorylation, IκB is multi-ubiquitinated and degraded by the 26S proteasome (*9*−*11*). The released NF-κB translocates to the nucleus where it activates a variety of inflammatory genes. The cytokine-inducible IκB kinase activity is contained in a 700 kDa complex, which carries two IκB kinases assembled as homo- or heterodimers, the 85 kDa IKK1 and the 87 kDa IKK2 (*12*−*15*). IKK1 and IKK2 are related serine kinases with an overall identity of 51%. Both kinases possess an N-terminal kinase domain, a central leucine zipper, and a C-terminal helix-loop-helix motif. They are so far the only kinases identified to be capable of simultaneously phosphorylating both degradation-relevant serines in IκBα and in IκBβ (i.e., at positions 32 and 36 in IκBα and at positions 19 and 23 in IκBβ [*16*, *17*]). Further, IKK2 may be considered as the dominant kinase since (i) it has been demonstrated to display a significantly higher IκBα phosphorylating activity than IKK1 when immunoprecipitated from overexpressing cells or reticulocyte lysates (*14*, *15*), (ii) the kinase activity of recombinant IKK2 has been shown to be 50−60-fold higher than that of IKK1 (*18*), and (iii) the IKK2-specific inhibitor acetyl salicylic acid appears to be sufficient to prevent TNF-induced NF-κB activation (*19*).

The IKK complex, in turn, can be phosphorylated and thereby activated either by the NF-κB inducing kinase (NIK) and/or by the mitogen-activated protein kinase/ERK kinase kinase-1 (MEKK-1). Both kinases are significantly homologous in their catalytic domain, and both belong to the class of mitogen-activated protein kinase kinase kinases (*16*, *20*−*22*). The importance of NIK as an upstream regulator of the

* Address correspondence to Dr. Jörg Eder, Novartis Pharma AG, S-386.943, CH-4002 Basel, Switzerland. Tel: ++41 61 3244678. Fax: ++41 61 3244046. E-mail: joerg.eder@pharma.novartis.com.

[1] Abbreviations: NF-κB, nuclear factor-κB; IκB, inhibitor of NF-κB; IKK, IκB kinase; TNF, tumor necrosis factor; DTE, 1,4-dithioerythritol; EDTA, (ethylenediamine)-tetraacetic acid; PMSF, phenylmethylsulfonyl fluoride; SDS, sodium dodecyl sulfate; tricine, *N*-[2-hydroxy-1,1-bis(hydroxymethyl)ethyl]glycine.

10.1021/bi990220t CCC: $18.00
Published on Web 04/21/1999

IKK complex is underlined by the fact that IKK-1 was independently isolated in a two-hybrid screen when NIK was used as a bait (*23*). NIK also appears to be contained in the biochemically purified IKK complex (*14*, *24*). However, recent results indicate that MEKK-1 may be an equally effective activator of the NF-κB pathway as compared with NIK: its overexpression leads to significant NF-κB activation in reporter gene assays, it can directly stimulate the IKK complex in vitro, and it can activate both IκB kinases in vivo (*16*). Other as yet identified components of the IKK complex are the NF-κB essential modulator (NEMO)/IKK-γ (*25*, *26*) and the scaffold forming IKK-complex-associated protein (IKAP) (*24*).

In support of the central role of the IKK complex in NF-κB regulation, we have recently demonstrated that all known IκB proteins occur preassociated with this complex (*27*). Yet, several reports suggest that different stimuli in different cell types can lead to distinct phosphorylation-dependent degradation kinetics of the various IκB isoforms (*8*, *28*−*30*). Here, we describe the kinetic characterization of IKK2 for the binding and phosphorylation of all four IκB variants. We show that in principle all IκB isoforms are equally good substrates for the enzyme, both in terms of association with the recombinant IKK2 homodimer and in terms of steady-state kinetic parameters for their phosphorylation. Further, the in vitro kinetic data correlate well with the degradation time course of the various IκB proteins in human umbilical vein endothelial cells after TNF stimulation.

EXPERIMENTAL PROCEDURES

Materials. All chromatographic media were from Pharmacia. Western blot detection reagents (ECL Plus) were purchased from Amersham International, and restriction enzymes and other DNA-modifying enzymes from Boehringer Mannheim Corp. Recombinant tumor necrosis factor was a kind gift of Dr. Paul Ramage (Novartis Pharma AG). Iodoacetyl LC biotin and streptavidin-coated 96-well microtiter plates were from Pierce. The baculovirus expression system BAC-TO-BAC HT was purchased from Life Technologies. All other reagents and chemicals were of the highest quality commercially available. Human umbilical vein endothelial (HUVE) cells were obtained from BIO Whittaker.

Expression and Purification of Recombinant IκB Isoforms. Recombinant IκBα (*31*) was generated as described (*27*). IκBβ1 (*32*), IκBβ2 (*33*), and IκBϵ (*7*) cDNA was produced from leucocyte RNA employing reverse transcription and amplified by polymerase chain reaction. Versions of the IκB isoforms that were 6×His-tagged were constructed by inserting a coding sequence for six successive histidine residues immediately upstream of the stop codon in the vector pET17b (Novagen, Inc.). Point mutations were generated with the QuikChange site-directed mutagenesis kit of Stratagene. The recombinant proteins were expressed in *E. coli* strain BL21 DE3 pLysS (Novagen, Inc.) according to the supplier's specifications and purified as follows (all steps at 0−4 °C). Three grams of wet cell pellet was resuspended in 10 mL of 50 mM Tris/HCl buffer at pH 8.0, containing 1 mM DTE, and sonicated on ice (3 × 1 min). The resulting homogenate was centrifuged in a Beckmann JA-20 rotor at 15 000 rpm for 15 min, and the IκB variant was precipitated from the supernatant by the addition of 30% (w/v) ammonium sulfate. After incubation for 15 min and centrifugation in a Beckmann JA-20 rotor at 14 000 rpm for 12 min, the pellet was dissolved in 20 mL of 50 mM Tris/HCl at pH 8.0, containing 1 mM DTE. The 6×His-tagged proteins were purified by affinity chromatography on nickel-nitrilotriacetic acid (NTA; Qiagen) resin following the supplier's specifications.

Expression in the Baculoviral System. IKK2 cDNA (*13*−*15*) was produced from leucocyte RNA employing reverse transcription and amplified by polymerase chain reaction. The coding sequence was inserted into the multiple cloning site (Not I/*Xba*I) of the pFASTBAC HTb vector (Life technologies), thereby adding a sequence to the 5′-end that encodes an N-terminal 6×His affinity tag. The construct was transposed to the recombinant bacmid DNA in the *E. coli* strain DH10 BAC, and the bacmid was isolated and transfected into Sf9 cells according to the supplier's specifications. The following steps were carried out at 4 °C. Approximately 5 g of wet cell pellet was resuspended in 35 mL of a 50 mM Tris/HCl buffer at pH 8.0, containing 500 mM NaCl, 10 mM mercaptoethanol, 100 μg/mL PMSF, and a mixture of other protease inhibitors (Boehringer Mannheim, "Complete"). After sonication of the cell suspension the volume was increased with the same buffer to 130 mL, and the homogenate was centrifuged in a Beckman 45 Ti rotor at 42 000 rpm for 2 h. The 6×His-tagged recombinant protein was purified from the supernatant by affinity chromatography on nickel-nitrilotriacetic acid (NTA; Qiagen) resin following the supplier's specifications. The eluted fractions containing the recombinant protein were dialyzed against a 50 mM Tris/HCl buffer at pH 8.0, containing 500 mM NaCl and 2 mM DTE.

Biotinylation of IκB and IKK2. Iodoacetyl-LC-biotin (Pierce) was used to covalently attach a functional biotin moiety to the different IκB proteins via their thiol groups. The labeling was carried out in 0.1 M Tris/HCl at pH 8.0 for 2 h at room temperature and the reaction quenched by the addition of DTE to a final concentration of 5 mM. Recombinant IKK2 was biotinylated via its amino groups using D-biotinoyl-ϵ-aminocaproic acid *N*-hydroxysuccinimide ester (Boehringer Mannheim) according to the manufacturer's instructions.

IκBα Serine 32 Phosphorylation Assay. The kinase reaction was done in 50 mM Tris/HCl buffer at pH 8.0, containing 10 mM $MgCl_2$, 100 nM okadaic acid, and 1 mM DTE. The substrates ATP and biotinylated IκBα were used at concentrations of 10 and 0.1 μM, respectively, and the reaction was started by the addition of the kinase. After 15 min at room temperature the reaction was terminated by the addition of EDTA and the reaction mixtures were transferred to streptavidin-coated 96-well microtiter plates. The phosphorylated IκBα was then detected using a phospho-specific IκBα (Ser32) antibody (New England Biolabs) in combination with a horseradish peroxidase conjugated anti-rabbit IgG antibody and employment of BM Blue POD substrate (Boehringer Mannheim). Finally, the absorbance of the wells was measured using a Spectra MAX 250 (Molecular Devices) plate reader at 450 versus 650 nm.

Native Molecular Weight Determination by Gel Filtration. Two-hundred microliters of 2 μM recombinant IKK2 was subjected to gel filtration chromatography on a Superdex 200

column in 25 mM Tris/HCl buffer at pH 8.0, containing 150 mM NaCl and 1 mM DTE. Prior to the experiment the column had been calibrated with proteins of known molecular weights: thyroglobulin (669 000); ferritin (440 000); catalase (232 000); aldolase (158 000); albumin (67 000); and chymotrypsinogen A (25 000). The eluted fractions were analyzed for the presence of IκB kinase activity as described above, and the presence of IKK2 protein in the fractions was directly visualized by sodium dodecyl sulfate−polyacrylamide gel electrophoresis and subsequent Coomassie Blue staining.

Interaction Analysis by Surface Plasmon Resonance. The interaction of recombinant IKK2 with the various IκB isoforms was measured by surface plasmon resonance using a BIA2000 instrument (Pharmacia Biosensor, Freiburg; ref *34*). Experiments were performed at 25 °C at a flow rate of 5 μL/min. The carboxyl groups of CM5 sensor chips (Pharmacia Biosensor) were activated by passing a solution of 0.05 M *N*-hydroxysuccinimide and 0.2 M *N*-ethyl-*N*′-(dimethylaminopropyl) carbodiimide over the sensor matrix for 7 min. Streptavidin was then coupled via its amino groups by applying it at 50 μg/mL in a 10 mM acetate buffer at pH 4.5. The streptavidin solution was applied for 7 min, and streptavidin binding resulted in an increase of the SPR signal by ∼2500 RU. Residual active groups were inactivated by exposure to 1 M ethanolamine for 7 min.

Purified recombinant IκB was biotinylated by iodoacetyl-LC-biotin (Pierce) on the thiol groups as described above. The biotinylated IκB isoform was then repeatedly applied to the streptavidin-coated sensor surface at 4 μg/mL in 10 mM HEPES at pH 7.4, 150 mM NaCl, 0.05% Tween 20, and 0.5 mM DTE (buffer A), resulting in an overall increase of the SPR signal by ∼1000 RU. After immobilization of the IκB through the biotin−avidin interaction, the nonspecifically bound proteins were washed off using a 25 mM Tris/HCl buffer at pH 8.0 containing 500 mM NaCl, 1 mM DTE, and 0.1% Triton X-100. Recombinant IKK2 in buffer A was passed over the immobilized IκB at stepwise increasing concentrations from 5 to 320 nM for 20 min each. To check for cooperative binding, we performed similar measurements using biotinylated IKK2 that was immobilized to the streptavidin-coated sensor surface and probed with recombinant IκB in free solution.

Determination of Kinetic-Binding Parameters. Both association and dissociation rate constants for the interaction of IKK2 with the α/β1/β2/ϵ isoforms of IκB were determined. Assuming pseudo-first-order kinetics with an excess of IKK2 in free solution over the immobilized IκB protein, the binding on the sensor surface can be described by the following equation:

$$dR/dt = k_a c(R_{max} - R_t) - k_d R_t$$

where dR/dt is the overall rate of binding of the kinase to the immobilized IκB isoform (expressed in resonance units [RU]/s), k_a is the association rate constant, k_d is the dissociation rate constant, c is the concentration of the IKK2 in free solution, R_{max} is the maximal amount of kinase bound to the sensor (expressed in RU), and R_t is the amount of kinase bound to the sensor surface at time t (expressed in RU).

This equation can be rearranged to

$$dR/dt = k_a c R_{max} - (k_a c + k_d) R_t$$

dR/dt (i.e., the slope of the binding curve) is thus a linear function of R_t with the slope $k_s = (k_a c + k_d)$. For a series of different kinase concentrations, these slopes k_s were determined and plotted against c. The slope of this function corresponds to the association rate constant k_a; the intercept with the y-axis corresponds to the dissociation rate constant k_d. For this analysis, a segment of the sensorgrams was used starting approximately 15−25 s after switching from buffer to kinase solution, thus excluding initial distortions due to injection and mixing.

Measurement of Intrinsic Fluorescence. Fluorescence excitation spectra were measured with a FluoroMax-2 spectrofluorometer (Jobin Yvon-Spex Instruments S. A., Inc., Edison, NY) at 20 °C with excitation at 280 nm. The excitation and emission monochromator slits were 0.5 and 1.175 mm, respectively. For determination of the IκB-binding sites on IKK2, a solution of 0.5 μM IKK2 (with respect to the monomeric polypeptide chain as determined both by the Bradford protein assay [*35*] and by titration of the ATP-binding sites) in 50 mM Tris/HCl at pH 8.0, 0.5 M NaCl, and 1 mM DTE was titrated with increasing amounts of IκBα (stock solution of 20 μM in the same buffer). The fluorescence emission of the protein solution was recorded at 338.5 nm for each titration point after equilibrium had been reached. The resulting titration curve was fitted according to the following equation:

$$F(x) = F_0 - (F_{min}/c_0(0.5)(K_D + c_0 + x - \sqrt{(K_D + c_0 + x)2 - 4c_0x} + F_x x$$

where F is the intrinsic fluorescence of the sample, c_0 is the total concentration of IKK2, F_0 is the fluorescence of the IKK2 solution in the absence of IκB, $-F_{min}/c_0$ corresponds to the fluorescence decrease as a consequence of IKK2/IκBα binding, K_D is the dissociation equilibrium constant for the IKK2/IκBα binding, x is the concentration of IκBα, and F_x is the fluorescence increase corresponding to the intrinsic fluorescence of IκB. The concentration of IκB-binding sites was determined from the intercept of the linear curve corresponding to the extrapolated initial fluorescence decrease with the asymptote to the fluorescence emission curve for higher concentrations of IκB.

Determination of Kinetic Parameters K_M and k_{cat}. Michaelis (K_M) and the catalytic rate (k_{cat}) constants were determined by using a radioactive in vitro phosphorylation assay. The phosphorylation of the different IκB isoforms by recombinant IKK2 was carried out at 20 °C in a total volume of 7.5 μL. IκB substrate concentrations were varied between 0.5 and 8 μM. The reaction was started by the addition of ATP with trace amounts of γ-^{33}P-labeled ATP and carried out for the indicated time periods. To stop the reactions, we added 4 μL of 500 mM EDTA and subjected the samples to SDS−polyacrylamide gel electrophoresis using 10% Tris-glycine gels. The gels were washed twice in 10% (v/v) acetic acid and 40% (v/v) methanol, dried, and exposed to a phosphoimager screen. The extent of phosphorylation was quantified by densitometric scanning, and initial reaction rates were determined from the increase of ^{33}P incorporation into IκB over the first 6−9 min of the kinase reaction. The K_M values

were calculated from Lineweaver−Burk plots, and k_{cat} values were determined from the following equation:

$$k_{cat} = K_M k_a - k_d$$

using the association (k_a) and dissociation (k_d) rate constants as calculated from the surface plasmon resonance experiments.

Induction of IκB Degradation in HUVE Cells by TNF Stimulation. The HUVE cells were cultured in Medium 199 (Life Technologies) supplemented with 10% fetal calf serum, antibiotics, and 1 ng/mL basic fibroblast growth factor. HUVE cells (2×10^5) at a density of 2.1×10^4 cells/cm^2 were stimulated with 100 ng/mL tumor necrosis factor for the indicated time periods. Stimulation was stopped by lysing the cells in 10% SDS. The lysates were subjected to SDS−polyacrylamide gel electrophoresis, and Western blot analysis was performed using IκB isoform-specific antibodies. An antiserum against recombinant IκBβ2 was provided by Neosystem (Strasbourg, France). All other primary and secondary antibodies were from Santa Cruz Biotechnologies, Inc. Detection was carried out using the ECL Plus chemiluminescence system.

RESULTS

Expression and Purification of IκB Isoforms and IKK2. All IκB isoforms, which were used in kinetic studies, were expressed as C-terminally His-tagged proteins in *E. coli* and purified to >90% purity as judged by SDS−polyacrylamide gel electrophoresis. Recombinant IKK2 was produced using a baculoviral expression system and purified via its N-terminal His-tag to apparent homogeneity. In the absence of IKK1 and expressed as a recombinant protein, IKK2 appears to form homodimers. To estimate to which extent IKK2 in this preparation occurs in dimeric form, we have determined its native molecular weight on a calibrated Superdex 200 gel filtration column. As judged from SDS−polyacrylamide analysis of the fractions, all IKK2 eluted from this column with a native molecular weight of about 200 kDa, corresponding to the dimerized state of the protein (Figure 1). Further, all detectable IκBα kinase serine 32 phosphorylating activity coeluted with this protein peak.

IKK2 Binds All Four IκB Isoforms with High Affinities. The IκBα/β1/β2/ϵ isoforms are preassociated with the cytokine-inducible IKK complex (*24*, *27*). To address the questions of (i) whether this preassociation is based on a direct high-affinity enzyme−substrate interaction between the IκB proteins and the IκB kinases in the complex and (ii) whether there is a preference for certain IκB isoforms over others, we studied the association and dissociation kinetics of the respective recombinant proteins employing surface plasmon resonance analysis. A thiol-reactive biotin derivative was covalently attached to the recombinant IκB proteins. The biotin derivative was added in a 1:1 molar ratio with respect to the recombinant protein to avoid strong interference between the biotinylation and the analyzed protein−protein interactions due to multiple biotinylated sites. Equal amounts of each IκB isoform were then immobilized on streptavidin-coated sensor surfaces via biotin−avidin interaction, and the nonspecifically bound proteins were washed off using a buffer of high ionic strength and 0.1% Triton X-100. The resonance signal after this washing procedure remained constant for all IκB isoforms, indicating that no immobilized IκB was leaking from the surface into the flow cell. The resonance signal after this washing step was taken as the baseline resonance for all following experiments.

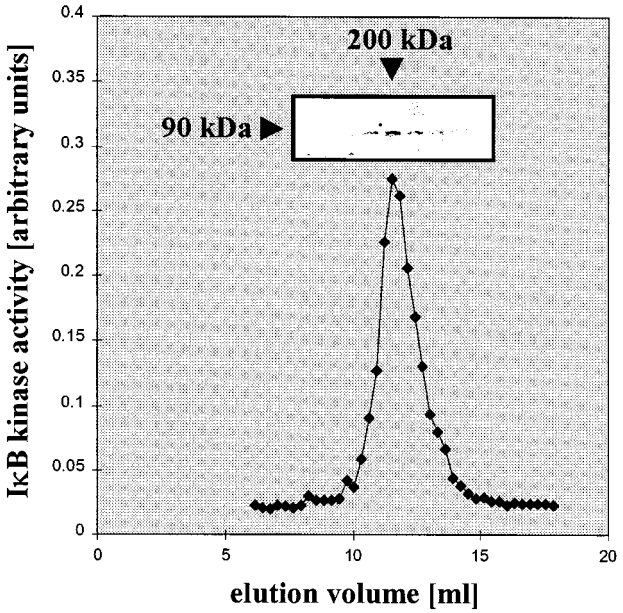

FIGURE 1: IKK2 is a homodimer. Analytical gel filtration of recombinant IKK2 was carried out on a calibrated S200 gel filtration column. The IκBα kinase activity contained in the eluted fractions is represented by the filled diamonds. The fractions were further analyzed by SDS−polyacrylamide gel electrophoresis and Coomassie Blue staining (inset). The estimated native molecular weight of the major IκB kinase activity, which correlates with the eluted IKK2 protein, is indicated by the filled arrowhead above the inset. The estimated molecular weight in SDS−PAGE is indicated by the arrowhead on the left of the inset.

For the initial binding experiment, recombinant IKK2 was injected at a concentration of 5 nM for 20 min and passed subsequently over a sensor surface coated only with streptavidin and then over a surface exposing an immobilized IκB isoform. The increase of the resonance signal on the IκB-coated surfaces (subtracted by the nonspecific signal increase on the streptavidin-coated surface) revealed a specific binding of the IKK2 to all four IκB isoforms (Figure 2). When the injection was finished and the running buffer was injected into the flow cell, the dissociation of the IκB-bound kinase complex on the sensor surface proceeded very slowly as followed by the decrease in the resonance signal. To omit harsh washing conditions for a regeneration of the baseline resonance, we carried out the following injections of IKK2 at higher concentrations without waiting for the dissociation of the enzyme−substrate complex on the sensor surface. The IKK2 concentrations were increased stepwise over 10, 20, 40, 80, and 160 to 320 nM with an injection time of 20 min for each concentration. As described in Experimental Procedures the association curves can be fit to an exponential function that corresponds to a bimolecular interaction. The exponential functions for the different IKK2 concentrations were extended to the theoretical baseline as depicted in Figure 2. By using these exponential functions, we calculated the association and dissociation rate constants (Table 1). Both rate constants are in the same range for all IκB isoforms and vary between 6.0×10^3 for IκBβ2 and 22.5×10^3 M^{-1} s^{-1} for IκBα for the association rate constants and between

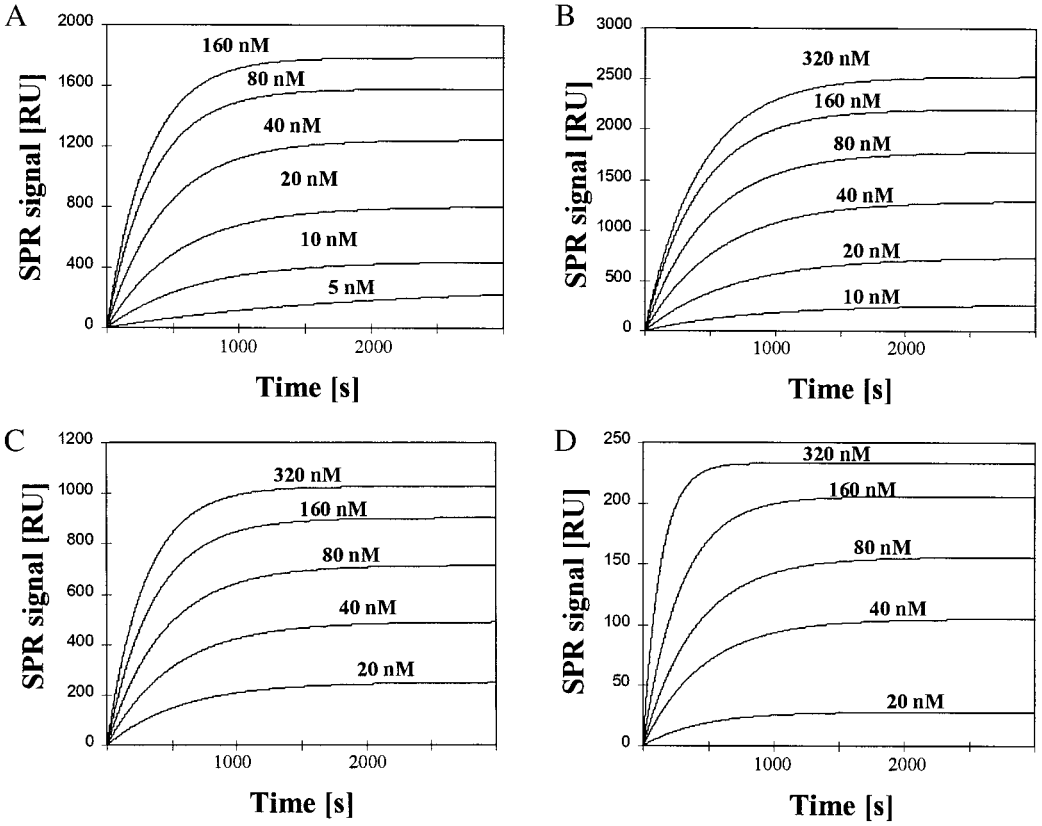

FIGURE 2: Interaction between IKK2 and the immobilized IκBα/β1/β2/ϵ isoforms analyzed by surface plasmon resonance. The biotinylated α, β1, β2, and ϵ isoforms (A, B, C, and D, respectively) of IκB were immobilized on streptavidin-coated BIA2000 sensor chips as described in Experimental Procedures. Recombinant IKK2 was injected into the flow cell at the concentrations indicated above the respective association curves. Nonspecific binding was measured in parallel on a streptavidin-coated surface and was subtracted from the resonance signal on the IκB-coated surfaces.

Table 1: Kinetics for the Interaction between IKK2 and the IκB Isoforms

IκB isoform	k_a (M^{-1} s^{-1})	k_d (s^{-1})	K_D[a] (M) = k_d/k_a
IκBα	22.5 (±2.5) × 10^3	1.25 (±0.15) × 10^{-3}	56 × 10^{-9}
IκBβ1	10.5 (±1.5) × 10^3	1.25 (±0.15) × 10^{-3}	119 × 10^{-9}
IκBβ2	6.0 (±1.0) × 10^3	1.75 (±0.15) × 10^{-3}	292 × 10^{-9}
IκBϵ	9.0 (±2.0) × 10^3	1.75 (±0.15) × 10^{-3}	194 × 10^{-9}

[a] The dissociation equilibrium constant K_D is the quotient calculated from the mean values of the dissociation and association rate constants (k_d and k_a).

1.25 × 10^{-3} and 1.75 × 10^{-3} s^{-1}, respectively, for the dissociation rate constants. These binding parameters suggest a stable enzyme−substrate association for all IκB/IKK2-binding partners with dissociation equilibrium constants (K_D) in the nanomolar range.

Alternatively, an inverted experimental setup was applied, that is, immobilizing a biotinylated form of the IKK2 and injecting a soluble, nonbiotinylated IκB isoform in free solution. The association and dissociation rate constants obtained from this inverted arrangement (see Figure 3 for IκBβ1 as an example) were very similar to the ones obtained above (Table 1), so that there are no apparent effects resulting from the immobilization of either binding partner. The mathematical form of the exponential functions to which the observed association curves can be fit excludes a cooperative effect in the subsequent binding of two IκB proteins to the immobilized IKK2 dimers (see below).

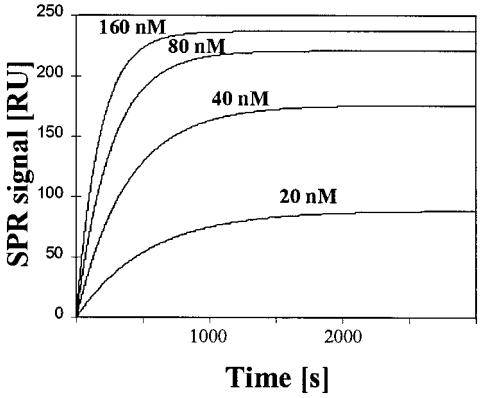

FIGURE 3: Interaction between IκBβ1 and the immobilized IKK2 analyzed by surface plasmon resonance. The biotinylated IKK2 was immobilized on a streptavidin-coated BIA2000 sensor chip. IκBβ1 was injected into the flow cell at the concentrations indicated above the respective association curves. Nonspecific binding was measured in parallel on a streptavidin-coated surface and was subtracted from the resonance signal on the IKK2-coated surface.

Stoichiometry of the Interaction between IKK2 and the IκB Isoforms. In the surface plasmon resonance assays, a noncooperative interaction between the IκB in free solution and the immobilized IKK2 homodimers was observed. However, the above experiments would only detect the existence of two IκB-binding sites on the IKK2 dimer if binding were cooperative. To address the issue of stoichiometry more directly, we studied the interaction of IKK2 with IκB by measuring the change in the fluorescence

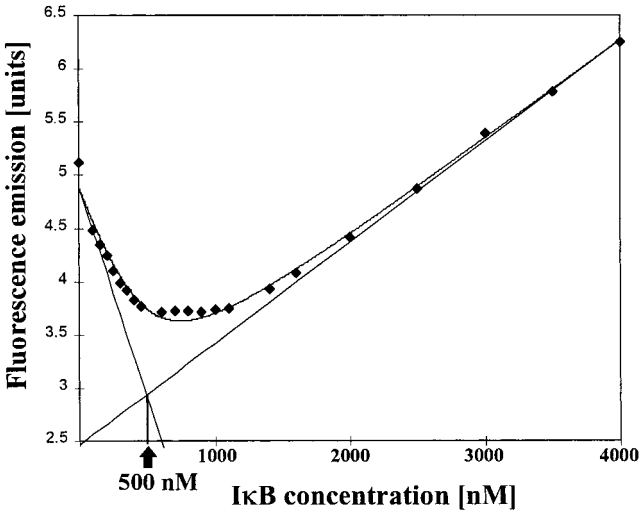

FIGURE 4: Titration of the IκB-binding sites on recombinant IKK2. A solution of 500 nM recombinant IKK2 in 50 mM Tris/HCl buffer at pH 8.0 containing 2 mM DTE and 0.5 M NaCl was titrated with the indicated amounts of IκBα. Fluorescence emission (black diamonds) was measured at 338.5 nm with excitation at 280 nm. The solid line represents a fitted curve (see Experimental Procedures) that takes into account the intrinsic fluorescence of both proteins, the fluorescence quenching upon binding, and the binding equilibrium of IκBα and IKK2. The concentration of IκB-binding sites was determined from the intercept of the linear curve corresponding to the extrapolated initial fluorescence decrease with the asymptote to the fluorescence emission curve for higher concentrations of IκB and is indicated by the arrow.

emission spectra of tryptophane and tyrosine residues in IKK2. Upon titration with IκB proteins, the IKK2 fluorescence spectrum was quenched and the fluorescence intensity was reduced by approximately 25%. An excess of IκB led to an increase in fluorescence due to the contribution of the IκB protein to the overall signal. The resulting titration curve fit to a curve that accounts for the fluorescence emissions of the individual proteins, the fluorescence quenching upon binding, and the equilibrium binding parameters (illustrated for IκBα in Figure 4). All IκB isoforms bound to the IKK2 homodimer stoichiometrically with respect to the enzyme's subunit concentration (0.5 μM). Therefore, each IKK2 dimer is capable of binding two IκB protein molecules.

Kinetic Parameters for IκB Phosphorylation. The surface plasmon resonance experiments indicate similar equilibrium dissociation constants (K_D) for the interaction of IKK2 with the four analyzed IκB isoforms. To determine if these similar dissociation constants are also reflected by the enzyme's catalytic efficiency for phosphorylation of the different IκB isoforms, we have determined the steady-state kinetic parameters, K_M and k_{cat}, in an in vitro phosphorylation assay. The initial velocities of IκB phosphorylation at IκB concentrations varying between 0.5 and 8 μM were determined by measuring the incorporation of radioactivity from trace amounts of γ-^{33}P-labeled ATP (total ATP concentration was 50 μM) into the IκB proteins. As illustrated in Table 2, the individual K_M values are between 1.7 for IκBα and 3.2 μM for IκBβ1 and thus only vary within a narrow range. The corresponding catalytic rate constants (k_{cat}) were calculated using the association and dissociation rate constants from the surface plasmon resonance measurements (see Experimental Procedures). The resulting values for k_{cat}/K_M values are all in the same range (22×10^3, 10×10^3, 5.4×10^3, and 8.5×10^3 s^{-1} M^{-1} for IκBα, IκBβ1, IκBβ2, and IκBϵ, respectively), indicating that per se all four IκB isoforms are phosphorylated by IKK2 with very similar catalytic efficiencies. Therefore, the various IκB isoforms are not only preassociated to IKK2 with similar affinities but also turned over with similar catalytic rates.

Table 2: Kinetic Parameters K_M and k_{Cat} for the Phosphorylation of the IκB Isoforms by IKK2

IκB isoform	K_M (M)	k_{cat}[a] (s^{-1})	k_{cat}/K_M[b] [(s^{-1} M^{-1})
IκBα	1.7 ($\pm$0.6) $\times$ 10^{-6}	3.7 $\times$ 10^{-2}	22 $\times$ 10^3
IκBβ1	3.2 ($\pm$1.1) $\times$ 10^{-6}	3.2 $\times$ 10^{-2}	10 $\times$ 10^3
IκBβ2	2.8 ($\pm$1.0) $\times$ 10^{-6}	1.5 $\times$ 10^{-2}	5.4 $\times$ 10^3
IκBϵ	2.6 ($\pm$0.4) $\times$ 10^{-6}	2.2 $\times$ 10^{-2}	8.5 $\times$ 10^3

[a] The k_{cat} value is calculated from the mean values of K_M, k_a, and k_d as described in the Experimental Procedures. [b] The catalytic efficiency k_{cat}/K_M is the quotient calculated from the mean values of the catalytic rate constant k_{cat} and the Michaelis constant K_M.

The Kinetics for Intracellular Degradation of the IκB Isoforms Correlate with the in Vitro Kinetic Parameters. Phosphorylation of IκB proteins by IKK on their degradation-relevant serine residues leads to ubiquitination and destruction of the proteins by the 26S proteasome. We have measured the intracellular degradation kinetics of all four IκB isoforms in human umbilical endothelial vein cells to analyze the physiological relevance of the above in vitro kinetic parameters. Cells were stimulated with TNF for the indicated time periods and, after stimulation, lysed and the lysates subjected to SDS−polyacrylamide gel electrophoresis. The degradation of the individual IκB proteins was followed by Western blot analysis using isoform-specific antibodies. As shown in Figure 5, IκBα, IκBβ1, and IκBϵ were degraded with similar kinetics while IκBβ2 appeared to have a slightly longer half-life after TNF stimulation. This finding may be explained by IκBβ2 having the highest K_D and lowest k_{cat} values of the IκB isoforms analyzed. Altogether, the rapid degradation kinetics correlate well with a model assuming the preassociation between IκB proteins and the IκB kinases of the IKK complex.

DISCUSSION

At present, it is still a matter of debate to which degree the individual members of the IκB protein family contribute to specific physiological responses and to differential regulation of the various NF-κB/Rel factors. The two IκB kinases 1 and 2, which target the degradation-relevant serines of the IκB isoforms, are contained in a 700 kDa protein complex. In this complex, it appears that IKK2 is the dominant IκB kinase for activation of NF-κB (i) when overexpressed and immunoprecipitated from cells or from reticulocyte lysates, it displays a significantly higher IκBα phosphorylating activity than IKK1 (*14*, *15*); (ii) recombinant IKK2 is 50−60 times more active on thioredoxin-IκBα(1−54) than recombinant IKK1 (*18*); and (iii) the anti-inflammatory agents acetyl salicylic acid and sodium salicylate bind to the ATP-binding site of IKK2 but not IKK1 and are able to prevent the TNF-induced NF-κB activation (*19*). We have employed recombinantly expressed homodimeric IKK2 as a model system to study the IκB/IKK2 association/phosphorylation kinetics. Fluorescence-based active site titration revealed the existence of two IκB-binding sites on each IKK2

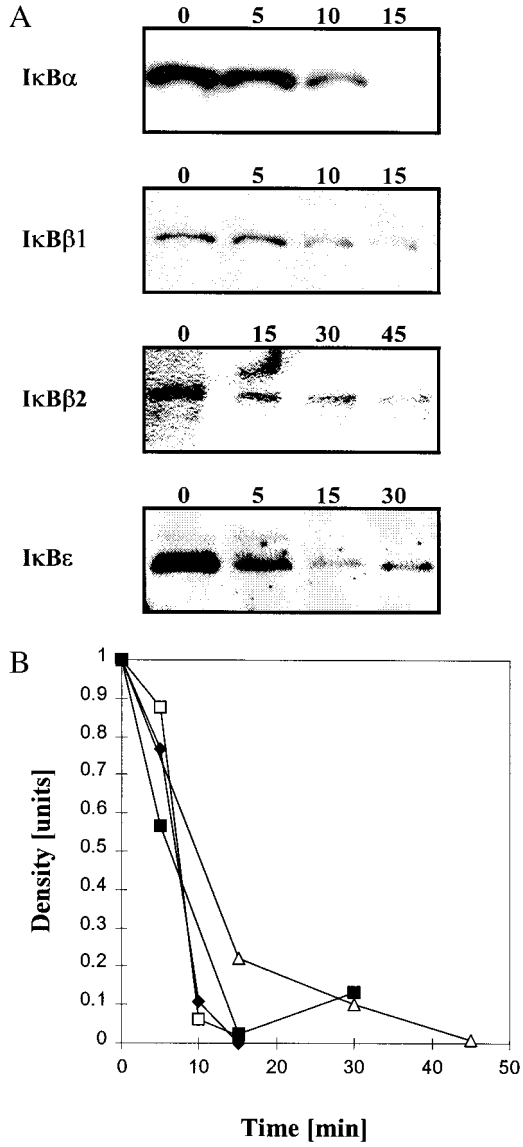

FIGURE 5: TNF-induced degradation of IκBα/β1/β2/ϵ in human umbilical vein endothelial cells. The human umbilical vein endothelial cells were stimulated with 100 ng/mL tumor necrosis factor α (TNF-α) for the time periods indicated above the insets. Following the stimulation period, the cells were lysed and the cellular lysates subjected to SDS−PAGE. (A) Degradation of the individual isoforms of IκB was visualized by Western blot analysis using isoform-specific antibodies. (B) Individual bands from part A were quantitated densitometrically and plotted versus time (IκBα, filled diamonds; IκBβ1, open squares; IκBβ2, open triangles; IκBϵ, filled squares).

dimer for all analyzed IκB isoforms. Since the physiological IKK complex also contains homo- or heterodimerically associated IκB kinases, we assume that each IKK complex likewise contains two IκB-binding sites. In this context it will be interesting to learn from future studies whether, for a given IKK complex, these sites can be occupied by different IκB isoforms at the same time or whether additional complex components lead to IκB-specific complexes.

Nevertheless, we found that all analyzed IκB isoforms display similar binding affinities to the IKK2 homodimer and are equally good substrates in terms of phosphorylation. The measured dissociation equilibrium constants, which range between 50 and 300 nM, explain the previous finding that all four IκB isoforms co-purify with the physiological IKK complex over several chromatographic steps (*24*, *27*). The also observed co-purification of the Rel family members RelA, RelB, cRel, p100, and p105 may thus be based on an indirect binding to the IKK complex mediated by the IκB proteins. Further, the preassociation of the IκB proteins with the IKK complex may contribute to the rapid onset of IκB phosphorylation and degradation after cytokine stimulation.

Previously, the K_M value for the phosphorylation of GST-IκBα by recombinant IKK2 has been determined to be 2.2 μM (*17*) and that for thioredoxin-IκBα(1−54) to be 1.3 μM (*18*). We found a similar K_M value for the phosphorylation of His-tagged IκBα by IKK2 (1.7 μM) and further found the K_M values for the phosphorylation of IκBβ1/β2/ϵ proteins to be in the same range. In addition, the k_{cat} values only vary between 1.5×10^{-2} s^{-1} for IκBβ2 and 3.7×10^{-2} s^{-1} for IκBα, which underlines the similar substrate quality of all analyzed IκB isoforms. It should, however, be noted that all K_M and k_{cat} values determined so far are apparent values, as each of the analyzed IκB isoforms possesses two major phosphorylation sites which both are phosphorylated simultaneously by the IκB kinases upon TNF stimulation (*4*−*8*); we determined the overall kinetic constants for the dual phosphorylation reaction. In addition, in our experiments the k_{cat}/K_M value for the phosphorylation of full-length His-tagged IκBα (22×10^3 s^{-1} M^{-1}) is about six times higher than the previously determined value, 3.5×10^3 s^{-1} M^{-1}, for the thioredoxin-IκBα(1−54) fusion protein (*18*). This may be explained by a C-terminal epitope in the full-length substrate that increases the catalytic efficiency of the phosphorylation.

The N-terminally phosphorylated forms of the IκB proteins can be distinguished from the non- or basally phosphorylated forms due to their slower migration in SDS−polyacrylamide gels (*5*, *7*, *36*). Since no accumulation of these phosphorylated IκB proteins was observed after TNF stimulation in human umbilical vein endothelial cells (Figure 5A), we assume that the N-terminal phosphorylation of the IκB proteins is rate-limiting for the cytokine-induced IκB degradation in these cells. Thus, the in vitro kinetics for the IKK2-dependent phosphorylation of the various IκB proteins can be compared with the intracellularly observed TNF-induced degradation of the respective IκB proteins. We find that the similar catalytic parameters for the diverse IκB isoforms are mirrored by the similar half-lives of the respective IκB proteins in human umbilical vein endothelial cells after TNF stimulation (Figure 5B). The slightly delayed degradation of IκBβ2 may somewhat be reflected by the highest K_D value and the lowest k_{cat} value among the isoforms analyzed. As the β1 and β2 isoforms of IκB only differ in their C-terminal regions, it is likely that a β1-specific site in this region increases the affinity for the IκB kinases.

Since all four IκB isoforms appear to be equally good substrates both in vitro and in HUVE cells, factors other than the phosphorylation rate should determine the isoform-specific regulation of IκB proteins which was observed in other cell lines (*7*, *8*, *28*, *33*). Perhaps the cell-type-specific association with particular Rel proteins improves or reduces the substrate qualities of the IκB isoforms. In this respect, it is interesting to note that GST-IκBα and GST-IκBβ fusion proteins are phosphorylated more efficiently in the presence of the p50/p65 heterodimer (*17*). Additional reasons for cell type-specific differences in the regulation of IκB proteins

might be their different cytosolic/nucleic distribution (*37*), other phosphorylation sites on Rel or IκB family members (*38*−*40*), or cell type-specific expression/basal turnover patterns of Rel/IκB proteins (*29*, *41*). Certainly, the molecular basis of the differential regulation in combination with the individual roles of the various IκB proteins will be one of the major areas for future studies to understand the basic concepts of NF-κB biology.

ACKNOWLEDGMENT

We thank Hermann Gram for critical reading of the manuscript and Brian P. Richardson for his constant support of this project.

REFERENCES

1. Baeuerle, P. A., and Baltimore, D. (1996) *Cell 87*, 13−20.
2. Baldwin, A. S. (1996) *Annu. Rev. Immunol. 14*, 649−681.
3. Verma, I. M., Stevenson, J. K., Schwarz, E. M., Van Antwerp, D., and Miyamoto, S. (1995) *Genes Dev. 9*, 2723−2735.
4. DiDonato, J. A., Mercurio, F., Rosette, C., Wu-Ii, J., Suyang, H., Ghosh, S., and Karin, M. (1996) *Mol. Cell. Biol. 16*, 1295−1304.
5. Traenckner, E. B., Pahl, H. L., Henkel, T., Schmidt, K. N., Wilk, S., and Baeuerle, P. A. (1995) *EMBO J. 14*, 2876−2883.
6. Whiteside, S. T., Ernst, M. K., LeBail, O., Laurent-Winter, C., Rice, N., and Israel, A. (1995) *Mol. Cell. Biol. 15*, 5339−5345.
7. Whiteside, S. T., Epinat, J., Rice, N. R., and Israel, A. (1997) *EMBO J. 16*, 1413−1426.
8. Weil, R., Laurent-Winter, C., and Israel, A. (1997) *J. Biol. Chem. 272*, 9942−9949.
9. Brown, K., Gerstberger, S., Carlson, L., Franzoso, G., and Siebenlist, U. (1995) *Science 267*, 1485−1491.
10. Alkalay, I., Yaron, A., Hatzubai, A., Jung, S., Avraham, A., Gerlitz, O., Pashut-Lavon, I., and Ben-Neriah, Y. (1995) *Mol. Cell. Biol. 15*, 1294−1301.
11. Chen, Z., Hagler, J., Palombella, V. J., Melandri, F., Scherer, D., Ballard, D., and Maniatis, T. (1995) *Genes Dev. 9*, 1586−1597.
12. DiDonato, J. A., Hayakawa, M., Rothwarf, D. M., Zandi, E., and Karin, M. (1997) *Nature 388*, 548−554.
13. Zandi, E., Rothwarf, D. M., Delhase, M., Hayakawa, M., and Karin, M. (1997) *Cell 91*, 243−252.
14. Woronicz, J. D., Gao, X., Cao, Z., Rothe, M., and Goeddel, D. V. (1997) *Science 278*, 866−869.
15. Mercurio, F., Zhu, H., Murray, B. W., Shevchenko, A., Bennett, B. L., Li, J. W., Young, D. B., Barbosa, M., Mann, M., Manning, A., and Rao, A. (1997) *Science 278*, 860−866.
16. Lee, F. S., Peters, R. T., Dang, L. C., and Maniatis, T. (1998) *Proc. Natl. Acad. Sci. U.S.A. 95*, 9319−9324.
17. Zandi, E., Chen, Y., and Karin, M. (1998) *Science 281*, 1360−1363.
18. Li, J., Peet, G. W., Pullen, S. S., Schembri-King, J., Warren, T. C., Marcu, K. B., Kehry, M. R., Barton, R., and Jakes, S. (1998) *J. Biol. Chem. 273*, 30736−30741.
19. Yin, M., Yamamoto, Y., and Gaynor, R. B. (1998) *Nature 396*, 77−80.
20. Lee, F. S., Hagler, J., Chen, Z. J., and Maniatis, T. (1998) *Cell 88*, 213−222.
21. Nakano, H., Shindo, M., Sakon, S., Nishinaka, S., Mihara, M., Yagita, H., and Okumura, K. (1998) *Proc. Natl. Acad. Sci. U.S.A. 95*, 3537−3542.
22. Ling, L., Cao, Z., and Goeddel, D. V. (1998) *Proc. Natl. Acad. Sci. U.S.A. 95*, 3792−3797.
23. Regnier, C. H., Song, H. Y., Gao, X., Goeddel, D. V., Cao, Z., and Rothe, M. (1997) *Cell 90*, 373−383.
24. Cohen, L., Henzel, W. J., and Baeuerle, P. A. (1998) *Nature 395*, 292−296.
25. Yamaoka, S., Courtois, G., Bessia, C., Whiteside, S. T., Weil, R., Agou, F., Kirk, H. E., Kay, R. J., and Israel, A. (1998) *Cell 93*, 1231−1240.
26. Rothwarf, D. M., Zandi, E., Natoli, G., and Karin, M. (1998) *Nature 395*, 297−300.
27. Heilker, R., Freuler, F., Pulfer, R., DiPadova, F., and Eder, J. (1998) *Eur. J. Biochem. 259*, 253−261.
28. Weil, R., Whiteside, S. T., and Israel, A. (1997) *Immunobiology 198*, 14−23.
29. Cheng, J. D., Ryseck, R., Attar, R. M., Dambach, D., and Bravo, R. (1998) *J. Exp. Med. 188*, 1055−1062.
30. Thompson, J. E., Phillips, R. J., Erdjument-Bromage, H., Tempst, P., and Ghosh, S. (1995) *Cell 80*, 573−580.
31. Haskill, S., Beg, A. A., Topkins, S. M., Morris, J. S., Yurochko, A. D., Sampson, J. A., Mondal, K., Ralph, P., and Baldwin, A. S. (1991) *Cell 65*, 1281−1289.
32. Lee, J. W., Choi, H. S., Gyuris, J., Brent, R., and Murray, B. W. (1995) *Mol. Endocrinol. 9*, 243−254.
33. Hirano, F., Chung, M., Tanaka, H., Maruyama, N., Makino, I., Moore, D. D., and Scheidereit, C. (1998) *Mol. Cell. Biol. 18*, 2596−2607.
34. Karlsson, R., Michaelsson, A., and Mattsson, L. (1991) *J. Immunol. Methods 145*, 229−240.
35. Bradford, M. M. (1976) *Anal. Biochem. 72*, 248−254.
36. Harhaj, E. W., and Sun, S. (1997) *J. Biol. Chem. 272*, 5409−5412.
37. Arenzana-Seisdedos, F., Thompson, J., Rodriguez, M. S., Bachelerie, F., Thomas, D., and Hay, R. T. (1995) *Mol. Cell. Biol. 15*, 2689−2696.
38. Naumann, M., and Scheidereit, C. (1994) *EMBO J. 13*, 4597−4607.
39. Imbert, V., Ruppe, R. A., Livolsi, A., Pahl, H. L., Traenckner, E. B., Mueller-Dieckmann, C., Farahifar, D., Rossi, B., Auberger, P., Baeuerle, P. A., and Peyron, J. (1996) *Cell 86*, 787−798.
40. Singh, S., Darnay, B. G., and Aggarwal, B. B. (1996) *J. Biol. Chem. 271*, 31049−31054.
41. Krappmann, D., and Scheidereit, C. (1997) *Immunobiology 198*, 3−13.

BI990220T